J. Phys.: Condens. Matter 5 (1993) 4527–4540. Printed in the UK

A ferromagnetic monolayer with model spin–orbit and dipole–dipole interactions

M B Taylor† and B L Gyorffy
H H Wills Physics Laboratory, Royal Fort, Tyndall Avenue, Bristol, UK

Received 19 February 1993

Abstract. We have considered a classical spin model of a ferromagnetic monolayer with model spin–orbit and dipole–dipole interactions, which provide competing perpendicular and in-plane anisotropies respectively. In particular we plot the zero temperature phase diagram, which features, as well as the expected perpendicular and in-plane ferromagnetic phases, a series of unexpected perpendicular antiferromagnetic phases, although these are most important for anisotropy parameter values higher than we would expect to see in real monolayers. A mean field theory at finite temperatures predicts the existence of a first-order perpendicular to in-plane reorientation transition of the magnetization for certain values of the parameters. Computer simulations of this system were attempted, but were unsuccessful because of the large correlation lengths arising. We draw the tentative conclusion that straightforward Monte Carlo and molecular dynamics simulation is not a practicable way to investigate this system, and note the important technical point that data parallelization of conventional Monte Carlo methods with infinitely long-range interactions is not possible.

1. Introduction

It was first pointed out by Néel [1] that breaking the translational symmetry of a magnetically isotropic material (by introducing a surface) leads to the possibility of magnetically anisotropic terms in the Hamiltonian (a magnetic surface anisotropy). Specifically, he noted that if the anisotropy is written in a suitably general form, the leading pairwise term is zero in the bulk of a cubic crystal, but not at its surface.

Néel's discussion was phenomenological. More recently a particular physical basis for the anisotropic terms involved has been considered [2–4] and calculated [5,6]. This magnetic surface anisotropy is thought to arise firstly from the dipole–dipole interaction, and secondly from the electron spin–orbit coupling. The dipole–dipole interaction will lead to an in-plane anisotropy, and the spin–orbit term may lead either to in-plane or to perpendicular anisotropy. Since this is a surface effect, it may best be observed in systems with a high surface-to-volume ratio. Experimentally this is likely to mean thin films or multilayers; theoretically it is convenient to examine a two-dimensional system (a monolayer). We therefore investigate a plane of spins, attempting to determine its behaviour as a function of the two types of anisotropy.

There are three important and much-studied limiting cases of this model:

(i) If the anisotropies are both removed we recover the 2D classical Heisenberg model. This has no magnetic order at non-zero temperatures since the ferromagnetic order is

† Present address: Institute of Physics Publishing, Techno House, Redcliffe Way, Bristol BS1 6NX, UK.

0953-8984/93/264527+14$07.50

destroyed by long-wavelength spin waves, as demonstrated by Mermin and Wagner [7, 8]. Various theoretical and simulation analyses have been performed on this system, see e.g. references [9–14].

(ii) If the anisotropy is such that the spins are confined to the plane they become two-dimensional and we have the 2D classical XY model which also lacks ferromagnetism, but features a Kosterlitz–Thouless transition [15, 16]. Simulations of this system have been reported in references [17–19]

(iii) In the limit of strong perpendicular anisotropy the spins become one-dimensional giving the 2D Ising model with a finite Curie temperature T_C.

To gain an idea of physically realistic values of these anisotropy strengths we use the first-principles calculations of Gay and Richter [5] and of Guo *et al* [6], and the experimental results of Gradmann [20].

Two previous studies motivate us particularly to examine this system: the low-temperature mean field work of Jensen and Bennemann [2] which treats the magnetization and dipole–dipole interactions in rather simplified ways, and the renormalization group work of Pescia and Pokrovsky [4]. Both predict the existence, for some values of the interaction constants, of a reorientation temperature T_R below the Curie temperature, above which the magnetization is driven entropically from a perpendicular to an in-plane direction. Some experimental evidence of such a transition has been reported [21–23] and the perpendicular ferromagnetic state is of great importance in the technology of high-density magnetic recording media.

2. Details of the model

In investigating this system we use the simplest model that can be expected to capture the physics of interest. We will study a Hamiltonian with terms representing exchange, dipole–dipole interaction, and spin–orbit anisotropy:

$$\mathcal{H} = \mathcal{H}_{ex} + \mathcal{H}_{dip} + \mathcal{H}_{so}$$
$$= -\frac{1}{2}J\sum_{\langle ij\rangle}\boldsymbol{\sigma}_i\cdot\boldsymbol{\sigma}_j + \frac{1}{2}\omega\sum_{ij}\left[\frac{\boldsymbol{\sigma}_i\cdot\boldsymbol{\sigma}_j}{r_{ij}^3} - 3\frac{(\boldsymbol{\sigma}_i.\boldsymbol{r}_{ij})(\boldsymbol{\sigma}_j.\boldsymbol{r}_{ij})}{r_{ij}^5}\right] - \lambda\sum_i(\sigma_i^z)^2 \tag{1}$$

where at each site i, at position $\boldsymbol{r}_i$, of a two-dimensional square lattice in the x–y plane is a classical Heisenberg spin (three-dimensional unit vector) $\boldsymbol{\sigma}_i = (\sigma_i^x, \sigma_i^y, \sigma_i^z)$, and where $\boldsymbol{r}_{ij} = \boldsymbol{r}_j - \boldsymbol{r}_i$, $r_{ij} = |\boldsymbol{r}_{ij}|$, and the symbol $\langle ij\rangle$ denotes summation over nearest neighbours only. The parameters of the model are thus:

- J strength of the pairwise short-range (nearest neighbour) exchange interaction
- ω strength of the pairwise long-range (r^{-3}) dipole–dipole interaction
- λ strength of the single site model spin–orbit term
- T temperature

This expression is effectively a discrete form of the Hamiltonian used by Pescia and Pokrovsky [4], and is an improvement on that used by Jensen and Bennemann [2, 3] in that it does not simplify the dipolar interaction by representing it as a single-site term.

The limiting cases mentioned in section 1 are achieved with the following values of the parameters:

2D Heisenberg:	$J > 0$	$\lambda = 0$	$\omega = 0$
2D XY:	$J > 0$	$\lambda = -\infty$	$\omega = 0$
2D Ising:	$J > 0$	$\lambda = +\infty$	$\omega = 0$

Physically, ω must be non-negative, providing an in-plane anisotropy. J and λ on the other hand may be positive or negative. We concern ourselves in this study only with the case $J \geqslant 0$, a ferromagnetic exchange, and $\lambda \geqslant 0$, the spin–orbit term providing a perpendicular anisotropy. These choices are motivated by our interest in the perpendicular ferromagnetic state. Note that of the limiting cases listed above this excludes the 2D XY model.

3. Ground states

By inspection of the Hamiltonian (1) some facts about the ground states of the system can be inferred.

We note first that, for the square lattice, the anisotropic terms in the Hamiltonian define no preferred direction within the plane so that states will be continuously degenerate with respect to azimuthal angle ϕ.

If J is large compared with the other energies in the system, then we expect a ferromagnetic state. Given a ferromagnetic system, if the in-plane anisotropy ω is large compared with the perpendicular anisotropy λ the state will be in-plane ferromagnetic, and if λ is large compared with ω it will be perpendicular ferromagnetic.

However, if λ and ω are both large compared with J we have a different situation: the high λ forces all the spins perpendicular to the plane causing the term $-(3/2)\omega \sum_{ij}(\sigma_i \cdot r_{ij})(\sigma_j \cdot r_{ij})r_{ij}^{-5}$ in the dipole–dipole interaction to vanish. The remaining part of the dipole–dipole interaction $+(1/2)\omega \sum_{ij}(\sigma_i \cdot \sigma_j)r_{ij}^{-3}$ acts like an antiferromagnetic term, and if ω is sufficiently large this will overcome the exchange term, resulting in a perpendicular antiferromagnetic state of some sort. Such a state will be highly frustrated, since the dipole–dipole interaction is long-ranged, so that every spin wants to be antiparallel to every other spin.

The exact nature of such an antiferromagnetic state is not immediately obvious. We expect two sublattices, one of spin up and one of spin down, which by symmetry will each occupy half of the lattice sites. To ascertain the geometry of these sublattices, computer simulations were performed, starting in a disordered state at high temperatures and cooling slowly to zero temperature (see section 6). The results of these simulations (i.e. the resulting zero-temperature states) are on their own somewhat inconclusive, since at low temperatures the system tended to settle into states which look glassy and metastable, but visual observation of graphical representations of them suggests the corresponding ordered states to which they may be close. This procedure is an alternative to the ground-state search method described by, e.g. Ducastelle [24]. For these large values of λ, in which the low temperature states feature entirely perpendicular spins, the observed ground states seem to fall into three categories, characterized as follows:

(i) all spins in the same direction (either up or down),

(ii) alternating stripes of up and down spins, of a characteristic width for given values of λ and ω,

(iii) a 'chequerboard' pattern of up and down spins.

We therefore investigate the energies of the corresponding sets of ordered states, which we label as indicated:

ZFERRO: perpendicular ferromagnetic state: $\sigma_i^z = +1 \quad \forall i$
CHECK: chequered antiferromagnetic state:

$$\sigma_i^z = \begin{cases} +1 & r_i^x + r_i^y = 2p \\ -1 & r_i^x + r_i^y = 2p+1 \end{cases}$$

STRIPEn: striped antiferromagnetic state:

$$\sigma_i^z = \begin{cases} +1 & 2pn+1 \leqslant r_i^x \leqslant 2pn+n \\ -1 & 2pn+n+1 \leqslant r_i^x \leqslant 2pn+2n \end{cases}$$

In the above $r_i = (r_i^x, r_i^y)$ is the lattice position of site i measured in units of lattice spacing, p represents any integer, and in all cases $\sigma_i^x \equiv \sigma_i^y \equiv 0$. Example STRIPE$n$ phases are illustrated in figure 1. We compare these with the state we expect for small values of λ:

XFERRO: in-plane ferromagnetic state: $\sigma_i \equiv (\sigma_i^x, \sigma_i^y, \sigma_i^z) = (+1, 0, 0)$

we have not distinguished between those states explicitly defined above and equivalent degenerate states.

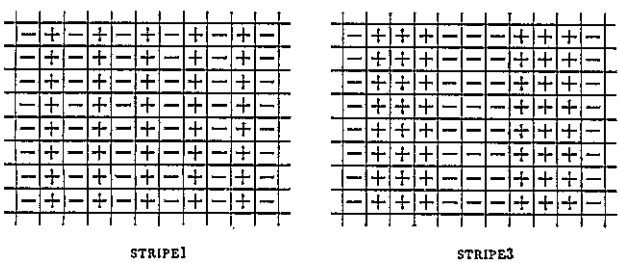

Figure 1. Pictures of example STRIPEn spin states, with $n = 1$ and $n = 3$. All spins are perpendicular, and the symbols + and − refer to up and down spins ($\sigma_i^z = +1$ and $\sigma_i^z = -1$) respectively.

The energies per site of these states are given as follows:

$$E_{\text{XFERRO}} = -2J - \frac{1}{4}A\omega \tag{2}$$

$$E_{\text{ZFERRO}} = -2J + \frac{1}{2}A\omega - \lambda \tag{3}$$

$$E_{\text{CHECK}} = +2J + C\omega - \lambda \tag{4}$$

$$E_{\text{STRIPE}n} = -\left(2 - \frac{2}{n}\right)J + S_n\omega - \lambda \tag{5}$$

where the values A, C and S_n are numerical constants depending on lattice geometry, defined using the spin states XFERRO, CHECK and STRIPEn respectively as:

$$\text{const}^{\text{state}} = \lim_{N\to\infty} \frac{1}{2N} \sum_{i=1}^{N} \sum_{j=1}^{N} \sigma_i^{\text{state}} \cdot \sigma_j^{\text{state}} \frac{1-\delta_{ij}}{|r_j - r_i|^3} \tag{6}$$

and these are calculated numerically, giving:

$$\begin{aligned} A &= +9.0336 \\ C &= -1.3230 \quad = (2^{-1/2}-1)A/2 \\ S_1 &= -0.4677 \\ S_2 &= +0.7908 \\ &\cdots . \end{aligned} \tag{7}$$

By manipulation of equations (2)–(5) we arrive at the zero-temperature phase diagram depicted in figure 2. The shaded rectangle near the origin represents the range of physically realistic values of ω and λ given in equation (13) and explained in section 4.

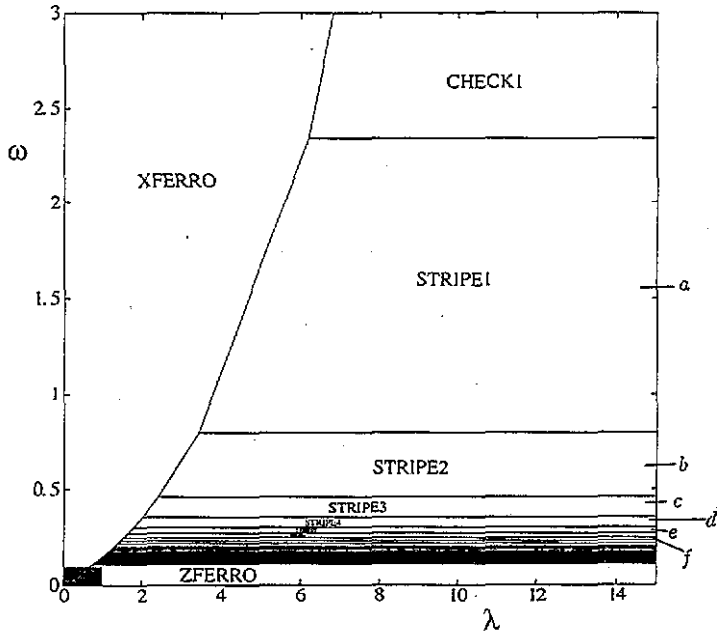

Figure 2. Zero-temperature phase diagram for the monolayer. STRIPE*n* phases are plotted for $n \leqslant 100$. *a*–*f*: stripes 1–6 respectively. The shaded rectangle near the origin indicates the physically realistic values for the model parameters (see section 4). All quantities are in units of J.

We present also an algebraic characterization of the phase diagram by giving the following equations of the boundaries of the in-plane ferromagnetic phase with the perpendicular ferromagnetic and chequered antiferromagnetic phases respectively:

XFERRO/ZFERRO:

$$\omega A = \frac{4}{3}\lambda \tag{8}$$

XFERRO/CHECK:

$$\omega A = \frac{4J}{\sqrt{2}-1}(\lambda - 4) \tag{9}$$

and the following expressions for the (λ, ω)

coordinates of the triple points:

XFERRO/CHECK/STRIPE1:

$$(\lambda, \omega) = J\left(4 + \frac{(\sqrt{2}-1)A}{(1-\sqrt{1/2})A + S_1}\,,\ \frac{4}{(1-\sqrt{1/2})A + S_1}\right) \tag{10}$$

XFERRO/STRIPEn/STRIPE$(n+1)$:

$$(\lambda, \omega) = J\left(\frac{2}{n+1} + \frac{A + 2S_{n+1}}{n(n+1)(S_{n+1} - S_n)}\,,\ \frac{4}{S_{n+1} - S_n}\left(\frac{1}{n} - \frac{1}{n+1}\right)\right). \tag{11}$$

We draw particular attention to the high-ω boundary of stability of the phase ZFERRO: we have plotted STRIPEn phase boundaries up to $n = 100$ in figure 2, but it is not clear to us what is the lowest value of ω at which a STRIPEn phase is stable. On the highly plausible assumption that S_n is monotonic in n we are then interested in the $n \to \infty$ limit of ω in equation (11), which ought more simply to be equal to the following expression:

$$\omega_{\max}^{\text{ZFERRO}} = \lim_{n\to\infty} \frac{4J}{n(A - S_n)}. \tag{12}$$

Using simple graphical methods to examine the first 100 values of S_n we have been unable to determine the asymptotic behaviour of $4J/n(A - S_n)$; in particular it does not appear to be related to n by a power law. However, it may be possible analytically or numerically to find an answer to this question. This point is clearly of great interest, since if $\omega_{\max}^{\text{ZFERRO}}$ is zero the perpendicular ferromagnetic phase is never a ground state of this system for finite ω. Even if it is not zero, its value is of importance for the behaviour of physically realistic materials.

The general features of the perpendicular antiferromagnetic phases CHECK and STRIPEn may be understood as follows: where the long-ranged antiferromagnetic tendency (ω) is very strong the system will be as antiferromagnetic as possible, resulting in the chequerboard pattern of CHECK. However, as the nearest-neighbour ferromagnetic exchange (J) becomes relatively more important, there is a tendency to reduce the number of up/down spin boundaries, while the long range of the dipolar interaction still acts to ensure that oppositely oriented spins exist at some distance away, favouring striped phases.

We have calculated energies for chequered states with squares larger than one lattice spacing, and none of these is stable, but we have no guarantee that there are not lower energy states which have not occurred to us. However, in view of the low temperature simulation results we think that this is unlikely.

The ground states in figure 2 except for the 2D Heisenberg case $\lambda = \omega = 0$, are not unstable to the long wavelength spin waves which destroy ferromagnetic order in that model according to the Mermin–Wagner theorem [7, 8]; the fluctuations are prevented from diverging by an energy gap of zeroth order in a wave vector proportional to λ [25] and one of first-order proportional to ω [26].

4. Physical values of the model parameters

In this section we put rough bounds on the values of the model parameters J, ω, λ which might correspond to real physical systems. As a first approximation we consider the values the parameters would take to model a monolayer of iron.

We can estimate the exchange interaction J by supposing that J is the same for an iron monolayer as for bulk iron, and that bulk iron is adequately approximated by a nearest-neighbour classical Heisenberg ferromagnet. Then by using a series expansion value for the Curie temperature of a BCC Heisenberg ferromagnet $k_B T_C = 2.06\,J$ [27] and an experimental value of Curie temperature $T_C^{Fe} = 1043\,K$ [28], we arrive at the estimate:

$$J^{Fe} \approx 40 \text{ meV}.$$

Theoretical [5, 6] and experimental [20] work suggest values of the other parameters $\lambda \approx 0.5\,\text{meV}$ and $\omega \approx 0.01\,\text{meV}$. These are rough estimates and values will clearly vary for different materials and environments, but we expect for all available materials:

$$\omega/J \ll 0.1 \qquad \lambda/J \ll 1 \tag{13}$$

and this region is indicated by the shaded rectangle near the origin of the zero-temperature phase diagram figure 2.

Most systems will fall well inside this region so it can be seen that of the phases plotted the most important are XFERRO and ZFERRO. It can therefore be seen that most of the phase diagram plotted corresponds to values of ω and λ which we do not expect to see in real monolayers, but we feel that the statistical mechanical interest of these unphysical regions is sufficient to justify depicting them.

We note also that cases of physical interest are far from the $\lambda = \infty$ 2D Ising limiting case and near to the $\lambda = 0$ 2D Heisenberg limiting case of the system, and we expect to see behaviour which is like a modified Heisenberg model, and unlike an Ising model.

5. Mean field theory

By making the substitutions:

$$\sigma_i = \langle \sigma_i \rangle + \delta\sigma_i \tag{14}$$

in the Hamiltonian (1) and discarding terms in $\delta\sigma_i \cdot \delta\sigma_j$, we can obtain a mean field Hamiltonian. Since we expect the ordered state to be ferromagnetic in the physical (small λ, small ω) region of the phase diagram we further assume homogeneity

$$\langle \sigma_i \rangle \equiv m = (m^x, m^y, m^z) \tag{15}$$

and thereby arrive at the following expression for the mean field free energy:

$$\begin{aligned} F &= -k_B T \ln \operatorname{Tr} e^{-\beta\mathcal{H}} \\ &= \frac{N}{2}\left[\left(4J + \frac{\omega A}{2}\right)(m^x)^2 + \left(4J + \frac{\omega A}{2}\right)(m^y)^2 + (4J - \omega A)(m^z)^2\right] \\ &\quad - k_B T N \ln \int_0^{2\pi} d\phi \int_0^{\pi} d\theta \sin\theta \exp\beta\left[\left(4J + \frac{\omega A}{2}\right) m^x \sin\theta\cos\phi\right. \\ &\quad \left. + \left(4J + \frac{\omega A}{2}\right) m^y \sin\theta\sin\phi + (4J - \omega A)\, m^z \cos\theta + \lambda\cos^2\theta\right] \end{aligned} \tag{16}$$

where N is the number of sites in the system, β is the reciprocal temperature $(k_B T)^{-1}$, and A is the constant defined in equation (7).

Given this free energy $F = F(m, J, T, \omega, \lambda)$, which can be evaluated and manipulated numerically, the behaviour of the system can be determined. In particular the Curie temperature T_C and the temperature of the first-order reorientation transition T_R can be located iteratively using the equations:

$$\left(\frac{\partial^2 F(T,m)}{\partial m^2}\right)_{m=0,\ T=T_C} = 0 \tag{17}$$

$$\left(F_\perp^0 - F_\parallel^0\right)_{T=T_R} = 0 \tag{18}$$

where $F_\perp^0$ and $F_\parallel^0$ are the values of the free energy when it is minimized with respect to m under the constraint of perpendicular and in-plane magnetization respectively.

Sample free energy surfaces in the regions of these transitions are illustrated in figure 3.

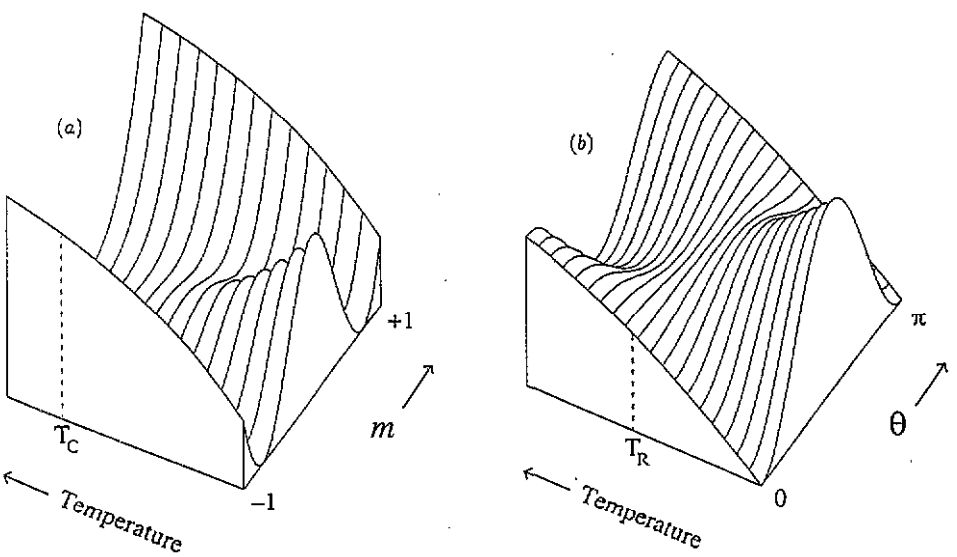

Figure 3. Mean field theory free energy surfaces (*a*) as a function of temperature and magnetization m; T_C is that temperature at which the two minima coalesce, and (*b*) as a function of temperature and angle θ of the magnetization from the vertical; T_R is that temperature at which the minimum switches from $\theta = 0$ to $\theta = \pi/2$.

The finite temperature mean field phase diagram determined using equations (17) and (18) is plotted in figure 4. We expect this to be qualitatively correct for values of ω and λ sufficiently small that the perpendicular antiferromagnetic phases are not important and sufficiently large that Mermin–Wagner fluctuations do not destroy the ferromagnetism at temperatures significantly above zero. Rather small values of ω and λ, even within the range given in equation (13), are plotted so that the former of these conditions is most likely to be satisfied (for indications that the latter is likely to be satisfied see figure 5 and its discussion) and because most real materials will probably lie in this range.

Solution of a mean field theory accommodating the large n STRIPEn phases (the only physical ones) would require considerable computational effort, and has not been attempted.

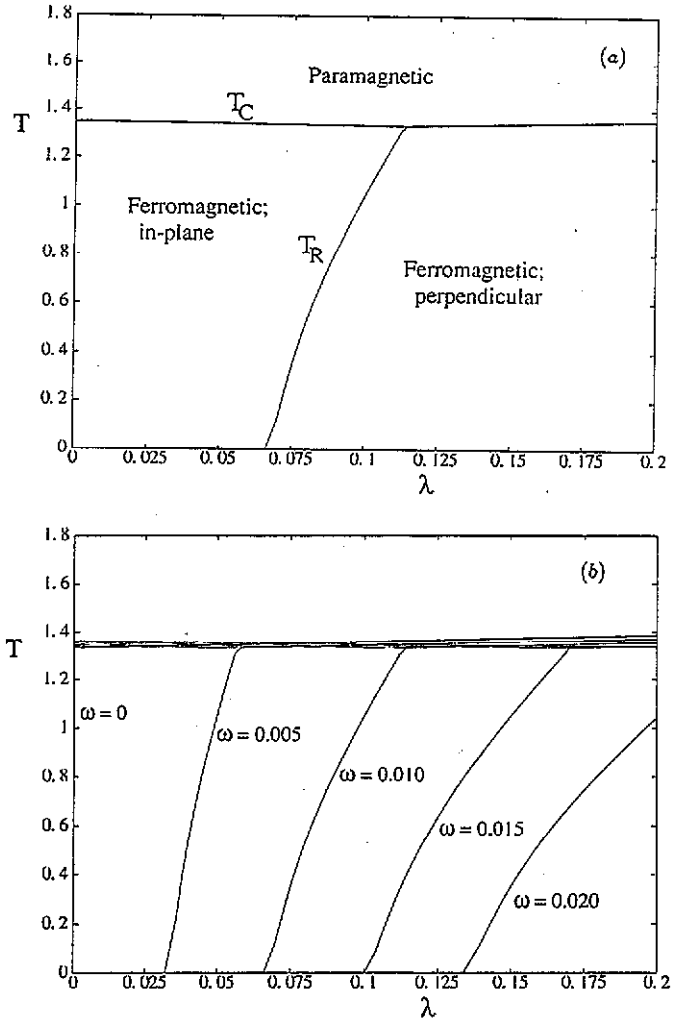

Figure 4. Mean field T against λ phase diagrams for small λ, ω monolayers. (*a*) shows the phases for $\omega = 0.01J$, and (*b*) shows the variation of the transition temperatures for some physically likely values of ω. All quantities are in units of J.

6. Computer simulation

The most powerful computing hardware available to us was a massively parallel (32 × 32 [8+1]-bit processors) AMT DAP 510C. The architecture of this machine is Single Instruction Multiple Data (SIMD), allowing efficient performance of an algorithm which exhibits data parallelism (the same operation may be performed on many data simultaneously), but not one which only exhibits algorithmic parallelism (several qualitatively different operations may be performed simultaneously).

For computer simulation of an idealized spin system such as this, the obvious method is Metropolis Monte Carlo [29,30], but a problem arises with data parallelization of the Monte Carlo algorithm.

Conventionally in Monte Carlo simulation, each step (modification of the spin state) requires making an alteration to a single spin and assessing the difference $\delta\mathcal{H}$ this makes in

the energy of the system. Providing that the change in energy associated with a spin σ_i at site i is not affected by the state of a spin σ_j at site j, then attempted updates can be made to the states of spins σ_i and σ_j simultaneously as required. However, if spins σ_i and σ_j are neighbours in terms of interaction range this is no longer possible, since the change in energy associated with the modification of spin σ_i is undefined if spin σ_j is simultaneously being modified so that it has no determinate state. Formally, spins σ_i and σ_j can be updated simultaneously only if:

$$\frac{\partial^2 \mathcal{H}}{\partial \sigma_i \partial \sigma_j} \equiv 0. \tag{19}$$

Thus, except in a (rather uninteresting) non-interacting spin system, it is not possible to update all spins in parallel. Some parallelization can be performed, however, by splitting the set $\mathbf{S}$ of all sites i into subsets $\mathbf{R}_l$ such that:

$$\forall i, j \in \mathbf{R}_l,\ i \neq j\ :\ \frac{\partial^2 \mathcal{H}}{\partial \sigma_i \partial \sigma_j} \equiv 0 \tag{20}$$

and then for each l, the spins at all the elements of $\mathbf{R}_l$ can be updated simultaneously. If this splitting can be done in such a way that the size of all the subsets $\mathbf{R}_l$ are multiples of the number of processors (in our case 1024) then the problem can be parallelized with maximal efficiency (i.e. without leaving any processors idle). Typically it is convenient to perform this decomposition into subsets so that all $\mathbf{R}_l$ are equivalent (mappable onto each other by translation) and as large as possible. A simple example of such a procedure is the case of nearest-neighbour interactions on a two-dimensional square lattice, in which case the lattice may be decomposed into two square sublattices $\mathbf{R}_1$ and $\mathbf{R}_2$ like the black and white squares on a chess board.

As the range of interactions becomes longer this lattice decomposition procedure becomes more difficult. An interaction of infinite range (one in which there is no cut-off) may be defined as follows:

$$\forall i, j \in \mathbf{S},\ \frac{\partial^2 \mathcal{H}}{\partial \sigma_i \partial \sigma_j} \not\equiv 0 \tag{21}$$

and in this case the largest subset $\mathbf{R}_l$ that can be selected is one site. We therefore conclude that data parallelization of conventional Monte Carlo simulation of systems with infinitely long-ranged forces is not possible.

This is an important fact which we have not seen pointed out elsewhere, and it will become more important as parallelization becomes a more common way of increasing computer power [31].

The only solution appears to be an 'unconventional' Monte Carlo in which each trial modification in the state of the system would consist of a small change in each of the spins rather than a large change in a single spin. Although this achieves data parallelism so that no processors need lie idle it will not allow a high rate of lattice updates per unit time, so it seems unlikely that it will be efficient. It may however deserve further investigation as a method of introducing spin waves rather than spin flips as trial spin state modifications.

For this reason we simulated using the molecular dynamics method [30] instead. Molecular dynamics is an inherently parallel method and does not present the same problems as Monte Carlo methods. For spin systems such as ours this involves introducing artificial

dynamics and is probably slightly less efficient than Monte Carlo methods, but seems otherwise satisfactory. Some test Monte Carlo simulations were performed (on a scalar processor) for comparison, and good agreement between the Monte Carlo and molecular dynamics results was found.

The simulation was performed on a square $L \times L$ cell with periodic boundary conditions, and an Ewald sum [32] was used to take account of its periodic images for evaluation of the long-ranged dipolar interaction energy.

Unfortunately, the simulations produced no conclusive results. The reason for this was that the correlation length ξ became larger than the linear dimension L of the simulation box at temperatures significantly above the Curie temperature. Simulation results at lower temperatures could then not be trusted, so that neither of the transitions of interest was represented reliably by the calculations. That this divergence could not be assumed to be in the immediate vicinity of T_C was demonstrated by the fact that ξ became comparable with L at $T \approx 0.75$ for the system $\omega = \lambda = 0$, the 2D Heisenberg model, for which T_C is known to be zero [7, 8]. It is therefore clear that accurate results are not available near enough the critical region for the usual finite size scaling methods to be of use.

Test simulations, not reported here (but see [33]), were performed in various regions of the phase diagram and in no case did they lead to reliable conclusions concerning this system. By careful analysis of the results, particularly of the spin–spin correlation function for the case $\lambda = \omega = 0$, it seemed likely that the simulation box size used was too small by several orders of magnitude. We therefore regretfully conclude that a computer simulation of this type is unhelpful in investigating this system at finite temperatures.

However, as mentioned in section 3 simulation results provided important indications about the ground states.

7. Discussion and comparison with other results

We are not familiar with any other work on this or similar systems which has identified the striped or chequered perpendicular antiferromagnetic phases shown in figure 2, although our simple energy considerations leave us in no doubt that they are more stable at low temperatures than the ferromagnetic phases usually assumed to dominate the phase diagram, and our simulations suggest that they are indeed ground states of the system. The lack of consideration of these phases in previous studies is no doubt a consequence of the fact that for values of the anisotropy parameters corresponding to real physical materials these phases are not obvious, but we reiterate from section 3 that it seems possible to us that the limit of large-striped phases extends down to the limit of small ω, in which case the perpendicular ferromagnetic state would not be stable for any finite value of ω. The fact that perpendicular ferromagnetism is seen experimentally could be compatible with this as a consequence of finite sample size, or of external fields applied for magnetization measurements which could act to stabilize the ferromagnetic phase.

Concerning finite temperature behaviour of the system, however, since simulations have failed to provide positive results, we have only the mean field ones of section 5. The mean field values for $T_C(\lambda, \omega)$ and $T_R(\lambda, \omega)$ shown in figure 4 can be compared with those predicted by other theories.

We consider first the work of Jensen and Benneman [2, 3]. Using a rather simplified mean field approach, they find a reorientation transition in agreement with our expectations, but they predict that the transition will, under certain circumstances, be continuous, proceeding via a canted magnetic state of which we see no evidence. They also predict

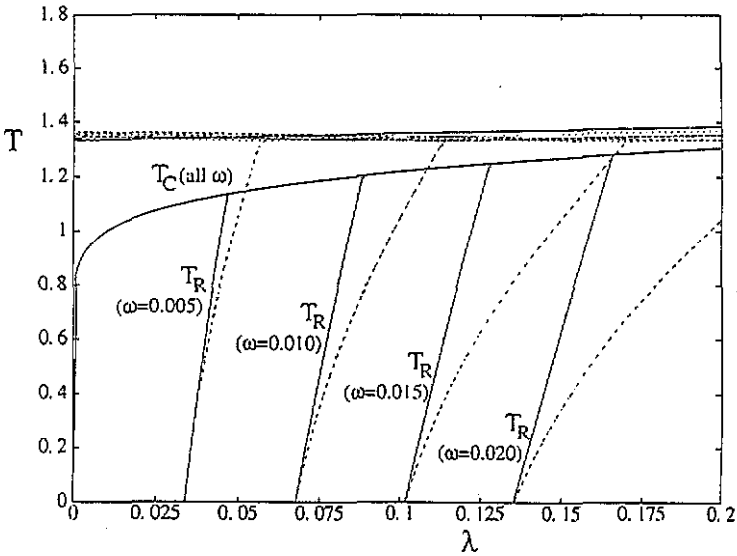

Figure 5. Polyakov renormalization group phase diagram for monolayer from [4] (labelled solid lines), compared with the mean field phase diagram from figure 4(*b*) (unlabelled broken curves). All quantities are in units of J.

that the magnetic order will decay in a range of 20–30 K around T_R. However, their model treats the dipolar and uniaxial anisotropies in the same way, effectively as single-site terms, merely reversing the sign between the two [3], and this is quite inadequate since the dipolar interaction only stabilizes the ferromagnetic state in virtue of its long-range nature. Our mean field theory treats the dipolar interaction correctly as pairwise and long-ranged and is in agreement with their prediction of a reorientation transition, although not with the other details mentioned above.

Pescia and Pokrovsky [4] have applied an adaptation of a renormalization group method developed by Polyakov [34]. This, unlike the simple mean field theory, correctly predicts the absence of finite temperature magnetization for the 2D Heisenberg model, so the crossover between this case and the small but finite ω, λ case is of particular interest to us. Expressions for the transition temperatures from this theory are as follows:

$$T_C = \frac{4\pi J}{8 + \ln J - \ln \lambda} \tag{22}$$

$$T_R = \frac{\pi J(4\lambda - 3A\omega)}{\lambda(\ln J - \ln \lambda)} \tag{23}$$

A phase diagram corresponding to these expressions is plotted in figure 5 where it is also compared with the mean field result already given in figure 4(*b*). Concerning the crossover between isotropic and anisotropic behaviour we see that it is very rapid: only very small values of λ are needed to stabilize the ferromagnetism even at high temperatures and to bring T_C to near its mean field value of the order of J. Thus we might suppose that the mean field theory which is unable to describe the instability of the pure isotropic case is a reasonably good approximation even for the rather small ω, λ of interest to us.

This is encouraging, but certainly there are doubts as to the validity of equations (22) and (23). It is quite clear that within this theory the dipolar anisotropy is not dealt with

correctly, since T_C is independent of ω, and in particular $(T_C)_{\lambda=0} \equiv 0$ for all values of ω, i.e. the dipolar interaction is not capable of stabilizing the ferromagnetic state. This is certainly not the case [26].

Furthermore, the recent work of Levanyuk and Garcia [35] claims that the Polyakov renormalization procedure is inappropriate for anisotropic spins at low temperatures. Levanyuk and Garcia investigated this model themselves using an ingenious low temperature expansion, and found no evidence for a reorientation transition. This is contrary to our expectations, based on the persuasive entropic arguments emphasized by Jensen and Benneman as well as our own mean field results. Since the approach of Levanyuk and Garcia is a low temperature one, the status of the mean field theory at high temperatures is somewhat uncertain. It may also be relevant for the comparison of results that the model explored here is classical in contrast to the quantum mechanical system of [35].

8. Conclusions

We have modelled a magnetic monolayer with a nearest-neighbour ferromagnetic exchange interaction, a long-range dipolar interaction, and a single site spin–orbit-type anisotropy.

We have mapped exactly most of the zero-temperature phase diagram and we have discovered, rather unexpectedly, a series of perpendicular antiferromagnetic phases which to our knowledge were not previously known to exist. These phases are most pronounced for values of the interaction parameters much larger than those we would expect for a real monolayer, but depending on the behaviour in the limit of large modulation length of the antiferromagnetic phase boundaries, which we have been unable to determine, these phases may replace the ferromagnetic perpendicular state as the ground states of some real monolayers.

We have failed to perform useful simulations of this system, and draw the tentative conclusion that straightforward Monte Carlo or molecular dynamics simulations of practicable sizes cannot be used to investigate it. We note also the important technical point that data parallelization of conventional Monte Carlo simulation of systems with infinitely long-range interactions is not possible.

We have formulated and solved, for physically realistic values of the anisotropy parameters, a finite temperature mean field theory which treats the dipolar interaction correctly as pairwise and long-ranged, and this exhibits an entropically driven first order reorientation transition at a temperature T_R from the perpendicular to the in-plane ferromagnetic state, and a Curie temperature T_C. In predicting a reorientation transition the mean field theory is in agreement with the previous work of Pescia and Pokrovsky [4] and of Jensen and Benneman [2, 3], but not with that of Levanyuk and Garcia [35]. Our disagreement with [35] may be a consequence of our use of classical, rather than quantum mechanical spins, although it should be remembered that the treatment of Levanyuk and Garcia is essentially a low temperature one. We feel on entropic grounds that the reorientation transition ought to exist [2], but have no proof that the mean field theory predicts the correct behaviour in this respect.

Acknowledgments

We would like to acknowledge several useful conversations with Dr M P Allen. MBT was financially supported by a SERC studentship and the calculations were carried out on the departmental DAP provided by the Computational Science Initiative.

References

[1] Néel L 1953 *Comptes Rendus* **237** 1468
[2] Jensen P J and Bennemann K H 1990 *Phys. Rev.* B **42** 849
[3] Jensen P J and Bennemann K H 1992 *Preprint*
[4] Pescia D and Pokrovsky V L 1990 *Phys. Rev. Lett.* **65** 20
[5] Gay J G and Richter R 1987 *J. Appl. Phys.* **61** 3362
[6] Guo G Y, Temmerman W M and Ebert H 1991 *J. Phys: Condens. Matter* **3** 8205
[7] Mermin N D and Wagner H 1966 *Phys. Rev. Lett.* **17** 1133
[8] Mermin N D 1968 *Phys. Rev.* **176** 250
[9] Shenker S H and Tobochnik J 1980 *Phys. Rev.* B **22** 4462
[10] Kawabata C and Bishop A R 1980 *Solid State Commun.* **33** 453
[11] Guttman A J 1978 *J. Phys. A: Math. Gen.* **11** 545
[12] Watson R E, Blume M and Vineyard G H 1970 *Phys. Rev.* B **2** 684
[13] Takahashi M 1987 *Phys. Rev.* B **36** 3791
[14] Fukugita M and Oyanagi Y 1983 *Phys. Lett.* **123** B71
[15] Kosterlitz M and Thouless D J 1973 *J. Phys. C: Solid State Phys.* **6** 1181
[16] Kosterlitz M 1974 *J. Phys. C: Solid State Phys.* **7** 1046
[17] Miyashita S, Nishimori H, Kuroda A and Suzuki M 1978 *Prog. Theor. Phys.* **60** 1669
[18] Tobochnik J and Chester G V 1979 *Phys. Rev.* B **20** 3761
[19] Van Himbergen J E and Chakravarty S 1981 *Phys. Rev.* B **23** 359
[20] Gradmann U 1986 *J. Magn. Magn. Mater.* **54–57** 733
[21] Pappas D P, Kämper K P and Hopster H 1990 *Phys. Rev. Lett.* **64** 3179
[22] Krebs J J, Jonker B T and Prinz G A 1988 *J. Appl. Phys.* **63** 3467
[23] Stampanoni M, Vaterlaus A, Aeschlimann M and Meier F 1987 *Phys. Rev. Lett.* **59** 2483
[24] Ducastelle F 1991 *Order and Stability in Alloys* (New York: North-Holland)
[25] Herring C and Kittel C 1951 *Phys. Rev.* **81** 869
[26] Stamps R L and Hillebrands B 1991 *Phys. Rev.* B **44** 12417
[27] Rushbrooke B S, Baker G A and Wood P J 1974 *Phase Transitions and Critical Phenomena* vol III, ed C Domb and M S Green (London: Academic)
[28] Massalski T B 1986 *Binary Alloy Phase Diagrams* (Menlo Park, OH: American Society for Metals)
[29] Metropolis M, Rosenbluth A W, Rosenbluth M N, Teller A H and Teller E 1953 *J. Chem. Phys.* **21** 1087
[30] Allen M P and Tildesley D J 1987 *Computer Simulation of Liquids* (Oxford: Oxford University Press)
[31] Charles D 1992 *New Sci.* **135** 1837 26
[32] Heyes D M 1981 *Surf. Sci. Lett.* **110** L619
[33] Taylor M B 1992 *PhD Thesis* University of Bristol
[34] Polyakov A M 1975 *Phys. Lett.* **59B** 79
[35] Levanyuk A P and Garcia N 1992 *J. Phys: Condens. Matter* **4** 10277